JMEPEG (2011) 20:1235–1241
DOI: 10.1007/s11665-010-9755-5

1059-9495/$19.00

Charge Weld Effects on High Cycle Fatigue Behavior of a Hollow Extruded AA6082 Profile

N. Nanninga, C. White, and R. Dickson

(Submitted May 7, 2010; in revised form July 16, 2010)

Fatigue properties of specimens taken from different locations along the length of a hollow AA6082 extrusion, where charge weld (interface between successive billets in multi-billet extrusions) properties and the degree of coring (accumulation of highly sheared billet surface material at back end of billet) are expected to vary, have been evaluated. The fatigue strength of transverse specimens containing charge welds is lower near the front of the extrusion where the charge weld separation is relatively large. The relationship between fatigue failure and charge weld separation appears to be directly related to charge weld properties. The lower fatigue properties of the specimens are likely associated with early overload fatigue failure along the charge weld interface. Coring does not appear to have significantly affected fatigue behavior.

Keywords aluminum, automotive, charge weld, coring, extrusion, fatigue, seam weld

1. Introduction

Extrusion of aluminum alloys is a non-steady-state process that can lead to variations in properties along the length of hollow extruded profiles. The physical and mechanical properties of extrusions can vary along their length due to variations in die line surface roughness, charge weld interfaces, billet coring, or thermal history (Ref 1-4). The effects of die line surface roughness on fatigue behavior in extruded AA6082 have been previously reported (Ref 5); but the effects of charge welds (interface between successive billets in multi-billet extrusions) and coring (accumulation of highly sheared billet surface material at back end of billet) on high cycle fatigue behavior have received relatively little attention.

The focus of this article is on the high cycle fatigue behavior of specimens taken from various locations along the length of an extruded AA6082 billet. The effects of variations in charge weld separation (as an indicator of charge weld quality) on fatigue properties are emphasized. To a lesser extent, the effects of billet coring are also evaluated and discussed.

2. Background

After a billet is extruded in commercial multi-billet extrusion processes, a portion of the billet butt remaining in the die is sheared (cut and removed), and the next billet is inserted into the die and extruded. This process can typically be repeated with a large number of successive billets before the die is changed. One reason for removing the butt of a partially extruded billet is to minimize the effects of "coring" (also called "back-end defects") on the extruded product. The origin of coring is in a thin layer that resides at the surface of a billet prior to extrusion (schematically represented as the black layer in Fig. 1a) (Ref 3, 6-8). Friction at the billet/container interface and variations in flow stress due to temperature gradients across the billet cross-section result in flow gradients both within the die and within the unextruded portion of the billet. These flow gradients cause material from the surface of the unextruded billet to accumulate at the center of the remaining unextruded portion of the billet. If the billet is not scalped, this "cored material" may be present in the last 66-85% of the extrusion (Ref 3, 6-8). In some cases, lubricants, oxides from heat treatment, or inhomogeneous distributions of intermetallics and second phase particles may reside near the surface of the billet, and accumulate in the cored material. In good extrusion practice, most of this contaminated material is removed by shearing the billet butt before the next billet is loaded for extrusion. In poor extrusion practice, the contaminated material remaining in the container can flow down the center of the extrusion during successive extrusion cycles to form a coring defect (Fig. 1b).

The location of the die exit port relative to the previously extruded material at the time of the billet insertion is easily identified by a "stop mark" on the extrusion surface, which serves as a reference point along the length of the extrusion (Fig. 1a). The stop mark lies in front of the unextruded material in the die and in the container. After a portion of the unextruded billet butt is sheared, and the following billet is inserted, an interface is formed between the two successive billets, and this interface is called a "charge weld." While the charge weld is initially planar and transverse to the extrusion direction (Fig. 1a), it becomes highly distorted as the trailing billet is extruded through the die (Fig. 1b). As extrusion of the trailing billet proceeds, the charge weld is distorted and stretched, approaching orientations parallel to the extrusion direction and eventually comes so close to the extrusion surface that it cannot

N. Nanninga, Materials Science and Engineering Department, Michigan Technological University, Houghton, MI 49931 and Materials Reliability Division, National Institute of Standards and Technology, Boulder, CO 80305; **C. White**, Materials Science and Engineering Department, Michigan Technological University, Houghton, MI 49931; and **R. Dickson**, Hydro Aluminum Technology Center, Holland, MI 49423. Contact e-mail: nanninga@boulder.nist.gov.

be easily distinguished from it, as shown schematically in the progression from sections "A" to "B" to "C" in Fig. 1.

Hollow profiles are formed by extruding a billet through a die containing die-ports and one or more mandrels that define the inside surface(s) of the profile. Each mandrel is held in place by one or more mandrel supports within the die, as illustrated at section "A" of Fig. 2. During extrusion, the billet must flow around the mandrel supports, rejoining downstream in the die weld chamber to form a "seam weld" before the fully formed extrusion exits the die. The seam welds will run along the entire length of a hollow extrusion. The number of seam welds in a given extrusion profile will equal the number of mandrel supports in the die.

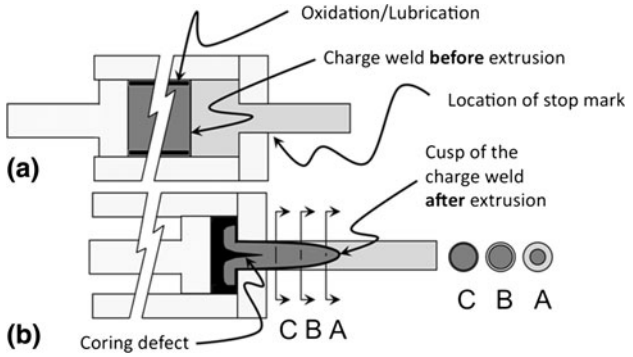

Fig. 1 Schematic illustrations of charge weld formation in a multi-billet extrusion. The leading billet has light shading and the trailing billet is dark. The charge weld is the interface between the two billets. Positions A, B, and C show how the relative amounts of the leading and trailing billet vary along the length of the extrusion in the transition region. Oxidized material (and lubricants, if used) at the billet surface (a) accumulates at the rear of the unextruded portion of the billet, and in some cases can flow back down the axis of the extruded billet to form a "coring" defect (b)

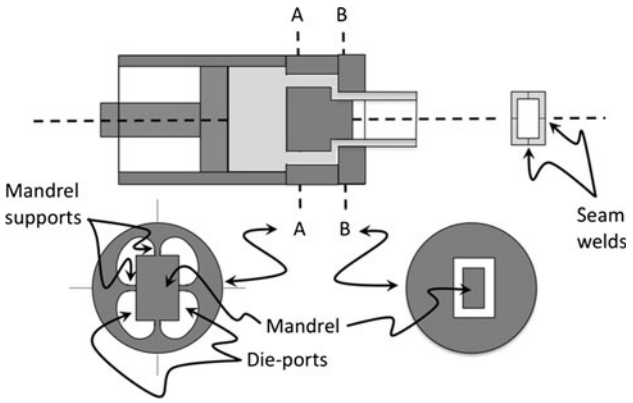

Fig. 2 Schematic illustration showing formation of seam welds in a hollow rectangular extrusion as the billet flows around mandrel supports (section A)

Hollow multi-billet extrusions will contain both seam welds and charge welds. The charge welds in hollow extrusions will be forced through each of the die-ports, and stretch in a manner analogous to that shown in Fig. 1, except that the charge weld will approach the interior surface of the extrusion and the seam welds, as well as the exterior surface of the extrusion at distances far from the stop mark.

The product from a single extrusion stroke in a multi-billet extrusion of a hollow profile can be divided (approximately) into four zones as shown in Fig. 3. Zone 1 represents the material from the leading billet that remained in the die and the billet container after the butt shearing operation. Zone 2 represents the transition between the two billets. At the cusp of the charge weld, the charge weld is only mildly stretched and is separated significantly from the surface or any adjacent seam weld. Throughout Zone 2, the charge weld is separate from the seam weld and the amount of stretching of the charge weld varies significantly. Zone 3 represents the bulk of the extrusion, and while it contains a charge weld, the charge weld in this region is so close to the adjacent surfaces and seam welds (and more importantly, so extensively stretched) that it has little influence on the properties of the extrusion. Material from zone 4 may be contaminated due to coring effects.

Stretching of the charge weld interface is associated with good quality solid state welds, leading to mechanical properties that are essentially the same as those in material not containing a charge weld (Ref 2). Multi-billet extrusions are sometimes observed to fail at or near the charge weld interface (Ref 2, 9, 10), and the tendency of the extrusion to fail at this location is greatest at locations close to the billet stop mark (Zone 2) where the charge weld has not been stretched significantly and the separation of the charge weld from the surface is relatively large. For many structural applications, this portion of multi-billet extrusions is scrapped.

In extrusion of heat-treatable aluminum alloys, billets are heated above the solutionizing temperature during extrusion and are then "press-quenched" immediately following extrusion. This allows the extruded material to be strengthened by age-hardening during postextrusion heat treatments. During

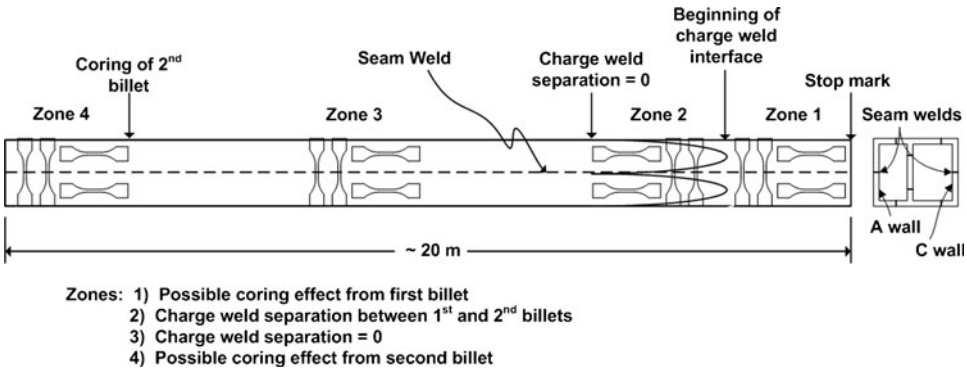

Fig. 3 Schematic illustration of specimens taken along the length of extruded product from second billet

billet butt shearing and billet loading operations in multi-billet extrusions, the material in Zone 1 may cool, and the temperature in portions of this material could fall below the solutionizing temperature for the alloy. This material may not age harden as effectively as material in Zones 2-4 that will not have cooled as much during the loading and butt shearing procedure.

All the abovementioned factors (coring, charge welds, seam welds and Zone 1 cooling during butt shearing) could influence the mechanical properties of extruded components. Nanninga et al. (Ref 11) have previously reported on the role of seam welds in Zone 3 of an AA6082 alloy extrusion on its fatigue behavior. That work concluded that any influence of seam and charge welds on fatigue behavior was primarily associated with increased die line roughness, and not the solid state welds themselves (Ref 5). Akeret (Ref 2) and van Rijkom (Ref 12) have reported degraded tensile properties in extrusions having large charge weld separations (Zone 2); but there has been very little study of the influence of either charge welds or coring on fatigue failure of extruded materials. The purpose of the study reported here is to examine the influence of seam and charge welds in Zone 2, and to a lesser extent of coring in Zone 4, on high cycle fatigue properties of an AA6082 hollow extrusion.

In general, fatigue failure of commercial aluminum alloys at ambient temperature occurs in three stages. First, a microscopic fatigue crack must nucleate via localized micro-plastic deformation. Once nucleated, the crack will grow as a result of the cyclic plasticity concentrated at the crack tip by the applied cyclic loading. When the fatigue crack has grown sufficiently, the specimen or component fails by overload failure.

High cycle fatigue failure ($N_f > 10^5$ cycles), is generally dominated by the crack nucleation process and/or stage I crack growth, which can occupy as much as 90% of the fatigue life (Ref 13). Fatigue crack initiation, in turn, depends on localized plastic deformation, which depends on the yield strength of the alloy and any microstructural factors that tend to localize plastic deformation at nominal loadings below the yield strength of the alloy. In extruded aluminum alloys containing charge welds, the presence of weak charge weld interfaces (e.g., as a result of inadequate stretching in Zone 2) could lead to premature fatigue crack nucleation or premature overload failure.

3. Experimental

The AA6082 material used in this study was obtained from the output of a single fully extruded billet, with the butt of one previous billet in the extrusion press so as to have representative charge welds and coring. The billet chemistry is shown in Table 1. During extrusion, the temperature of the extruded material will rise above the solid solution temperature due to heat generated by mechanical work. Because the alloys are solutionized, the extrusion was spray quenched with water upon exiting the die. The extruded profile in this study was a hollow rectangle with one center support, as shown in Fig. 3. The A and C walls of the profile contained a seam weld through the center of the wall. These walls were cut from the profile cross-section and aged at 185 °C for 5 h.

Following the aging treatment, fatigue and tensile specimens were CNC milled from the walls to dimensions conforming to ASTM E466 standard. The specimens had a constant gauge length of 10 mm and a width of 5 mm, with the thickness of the specimens depending on wall thickness (2.5 and 2.7 mm for the top (A) and bottom (C) walls, respectively). The faces of the specimens, with the exception of the milled surfaces, retained the as-extruded surface finish and the roughness of the extruded profile did not vary significantly along the length of the extrusion. The arithmetic average roughness of four scans taken on each of the extrusion walls was 2.23 ± 1.19 μm at the front of extrusion and 2.27 ± 0.68 μm at the back end of the extrusion. All fatigue testing was performed in load control at a stress ratio of 0.1 on a servo-hydraulic 90 KN testing machine. The frequency of each test was 20 Hz. Tensile tests were conducted using a screw driven test frame and specimens similar to those tested under fatigue conditions.

The results presented here are for fatigue and tensile specimens taken from Zones 1, 2, and 4 of the extrusions. Some longitudinal and transverse specimens contained extrusion welds within the center of the gauge section. Specimens cut transverse to the extrusion direction from the top (A wall) and bottom (C wall) contained centrally located welds (see Fig. 3). The different types of specimens and specimen nomenclature are provided in Table 2. Specimens from Zones 1, 2, and 4 of the AA6082 extrusion are compared with previously reported results from Zone 3 of the same extrusion (Ref 11). Because the main focus of this study is on the effect(s) of charge welds having large separations from the adjacent seam weld, most of the results are for transverse (T) specimens. Specimen microstructures were evaluated using standard metallographic techniques and fracture surfaces were characterized by scanning electron microscopy.

Table 1 AA6082 alloy chemistry

Analysis, wt.%								
Si	Fe	Cu	Mn	Mg	Cr	Zn	Ti	Al
0.95	0.20	0.03	0.52	0.58	0.14	0.02	0.02	Bal.

Table 2 Specimen nomenclature

Specimen type	Location	Specimen ID
Longitudinal no-weld	Zone 1	L-NW(1)
Transverse seam weld	Zone 1	T-W(1)
Longitudinal charge weld	Zone 2	L-CW(2)
Transverse charge weld	Zone 2	T-CW(2)
Longitudinal no-weld (a)	Zone 3	L-NW(3)
Transverse seam weld (a)	Zone 3	T-W(3)
Longitudinal no-weld	Zone 4	L-NW(4)
Transverse seam weld	Zone 4	T-W(4)

(a) Previously reported (Ref 11)

4. Results

Figure 4 shows etched and anodized cross sections normal to the extrusion direction for two AA6082 samples, one (a) located about 2 m from the stop mark and the other (b) located about 6.5 m from the stop mark. In Fig. 4(a), the charge weld is well separated from both the seam weld and the surfaces of the

extrusion. Figure 4(b) shows a higher magnification transverse optical micrograph of a seam weld in AA6082. The Mn in AA6082, and the high concentration of Si in this alloy, led to the formation of dispersoids that restrict recrystallization. Only the near surface regions of the extrusions are recrystallized, while the core retains a fibrous structure with grains that are highly elongated in the extrusion direction. It is noteworthy that the thickness of the recrystallized layer in AA6082 is greater at the seam weld than at other locations in the profile cross-section. In Fig. 4(b), the separation between the seam and the charge weld is essentially zero. Once the charge weld separation becomes zero and recyrstallization occurs across the interface, the charge weld becomes indistinguishable.

Figure 5 shows the charge weld separation from the seam weld plotted against distance from the stop mark for the A and C walls. There is very little difference between charge weld separations for A and C walls, and the charge weld separation decreases to zero at distances greater than about 2.5 m from the stop mark. The portion of the extrusion between ~1 m and ~2.5 m from the stop mark corresponds to Zone 2 in Fig. 1. Material less than ~1 m from the stop mark corresponds to Zone 1, and material more than ~2.5 m from the stop mark corresponds to Zones 3 and 4. There is no clear cut transition from Zone 3 to 4 but if coring is present in the extrusion, it should be most evident in the last 10-30% of the extrusion (Ref 3, 7, 8).

Since the specimen gauge length was only 10 cm, specimens taken transverse to the extrusion direction with charge welds in the gauge section were taken at approximate locations between 125 and 225 cm from the stop mark. The charge weld separation for these specimens varied from 0.5 to 8 mm. Since the gauge width of the specimen was 5 mm, specimens taken longitudinal to the extrusion direction with charge welds present in the gauge section were cut at approximately 160 to 225 cm from the stop mark.

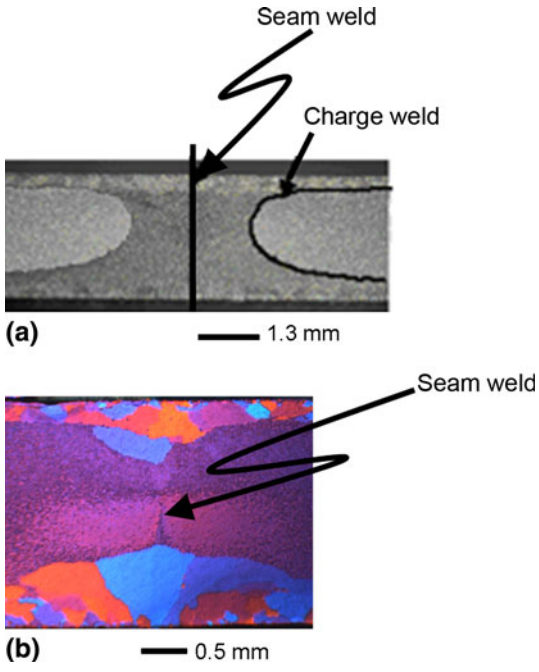

Fig. 4 Macrophotographs showing charge and seam welds in transverse cross-sections of two specimens from the extrusion. (a) An etched cross-section at ~2 m from the stop mark (Zone 2), and (b) an anodized cross-section at ~6.5 m from the stop mark (Zone 3)

4.1 Tensile Properties

Figure 6 compares the tensile properties of transverse and longitudinal specimens from Zones 1, 2, and 4 of the AA6082 alloy extrusion with previously reported properties of transverse (weld) and longitudinal (no-weld) specimens from Zone 3 of the same extrusion. The tensile and yield strengths in Zone 3 are generally slightly higher than for Zones 1, 2, or 4, but not dramatically so. The tensile elongations for Zones 1, 2, and 4 are also somewhat greater than for Zone 3, as might be expected for slightly weaker materials. The decreased strength for the L-NW(1) specimens could result, at least in part, from incomplete solutionizing (or high temperature aging) of material from the butt of the first billet extruded in the die, as discussed previously.

Coring, if present in this extrusion, would be expected to diminish the tensile ductility (while possibly elevating the strength slightly) of material in Zones 1 and 4. In fact, the opposite trend is observed in Fig. 6, suggesting little, if any, coring effect in the extrusion.

Previous studies have shown a correlation between charge weld separation and loss of mechanical integrity for hollow extrusions (Ref 2, 3, 12). The absence of any clear evidence of weakness in Zone 2 suggests that careful butt shearing and extrusion practice can yield mechanically sound material, at least as far as monotonic uniaxial tensile properties are concerned. Examination of the fractured tensile specimens indicated that none of the T-CW(2) specimens failed along the charge weld interface. These results verify the integrity of tensile properties for the charge welds in the hollow extrusions used for this study. The fatigue behavior of transverse specimens containing charge welds did not exhibit similar results, however.

4.2 Fatigue Behavior

Stress-life results for specimens taken longitudinal to the extrusion direction are shown in Fig. 7. Baseline L-NW Zone 3 results that were previously reported are presented as a solid curve (Ref 11). For the L-NW specimens from Zones 1 and 4 as well as L-CW specimens (Zone 2), results are shown as data

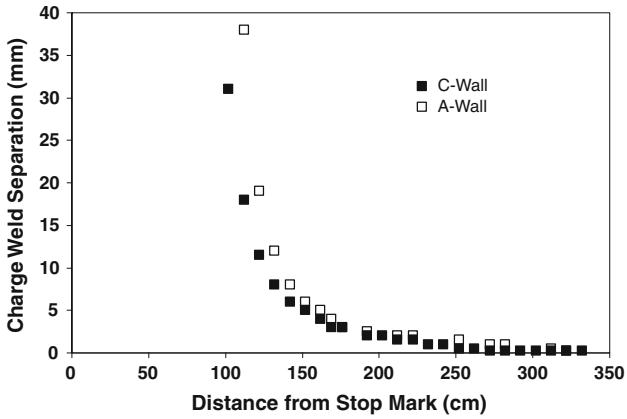

Fig. 5 Separation between charge weld interfaces as a function of distance from the stop mark (C wall is thicker (~2.7 mm) bottom profile wall, A wall is thinner (~2.5 mm) top profile wall)

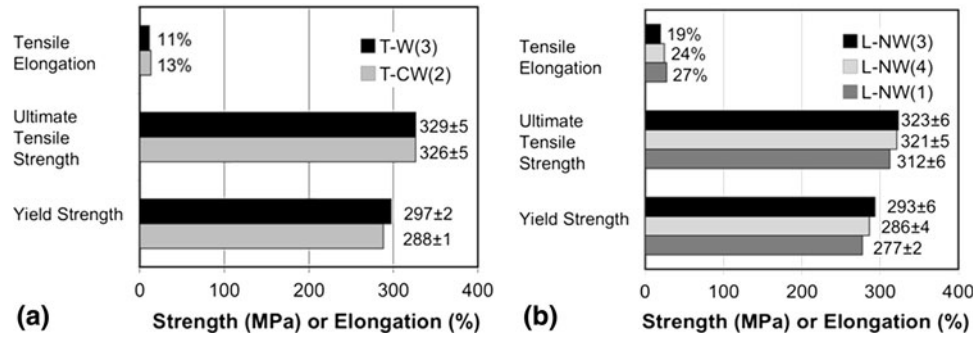

Fig. 6 Tensile properties of transverse (a) and longitudinal (b) specimens from Zones 1, 2, and 4 compared with properties from Zone 3 (three tests were performed for each variable and tensile property averages and standard deviations are provided next to each bar)

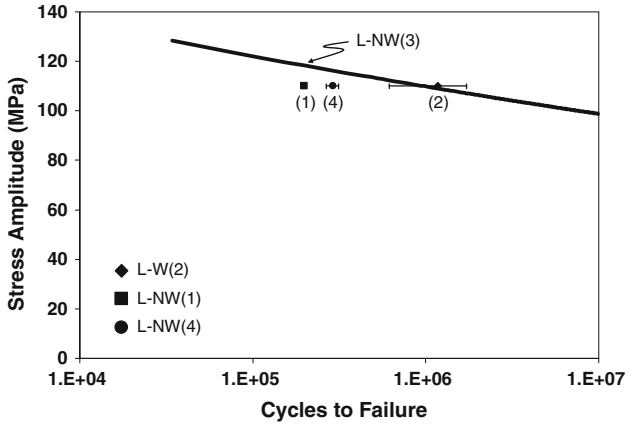

Fig. 7 Fatigue data from longitudinal specimens taken from Zones 1, 2, and 4 (solid trend line is from Zone 3 L-NW Ref 11). Data points represent averages from 3 to 5 specimens tested at stress amplitude of 110 MPa and error bars represent the standard deviation in fatigue lives of those specimens (standard deviations range from 3.6×10^3 cycles for Zone 1 specimens to 5.5×10^5 cycles for Zone 2 specimens)

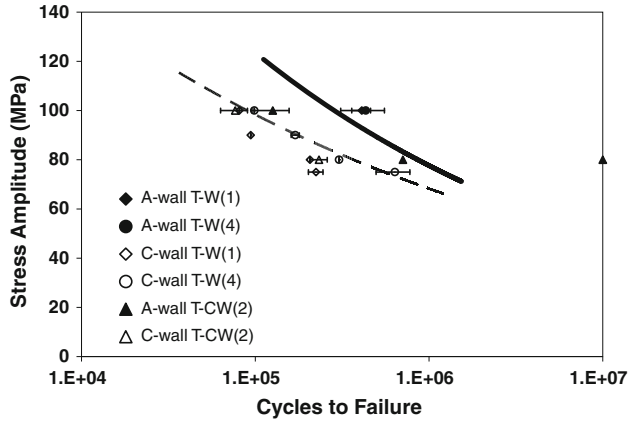

Fig. 8 Fatigue lives of transverse specimens. Solid and dashed trend lines represent previously reported fatigue data for T-W(3) specimens from the A and C wall's, respectively. Error bars represent standard deviations where repeat specimens were tested (standard deviations in figure range from a minimum of 1.8×10^4 for T-W(4) C-Wall specimens test at σ_A of 90 MPa to a maximum of 2.8×10^5 for T-W(4) C-wall specimens test at σ_A of 75 MPa)

points at 110 MPa, with error bars indicating standard deviations. From the L-CW(2) results, it appears that charge weld interfaces oriented longitudinally to the loading direction (Fig. 1) have little effect on fatigue life under uniaxial loading conditions. The average fatigue life of specimens taken from Zone 2, at stress amplitude of 110 MPa, is very close to the trend line for Zone 3 L-NW specimens. The fatigue lives of specimens taken from the front and the back of the extrusion (Zones 1, 4) consistently fall below the trend line for Zone 3 specimens, however. While the results for Zone 4 specimens are reduced, they are near the lower edge of the scatter band for results from Zone 3 (Ref 11). The fatigue life of Zone 1 specimens are further reduced from that of Zone 3 specimens, but this reduction in fatigue life correlates well with the reduction in yield strength of specimens taken from Zone 1, which may have not have been completely solutionized in some locations prior to quenching. The nominal ratio of stress amplitude to yield stress, at the average life of the specimens from Zone 1 (≈200,000 cycles), is essentially 0.40 for both Zone 1 and 3 L-NW specimens.

Fatigue results for transverse specimens from the top (A wall) of the extruded profile are presented in Fig. 8 as filled symbols (Zones 1, 2, and 4) and a solid curve (Zone 3). Specimens from Zones 1 and 4 were tested at only 100 MPa, and exhibited fatigue lives that were actually statistically better than their corresponding Zone 3 specimens. The fatigue crack initiation mechanisms for T-W specimens from Zones 1 to 4 were similar to those from Zone 3, where fatigue cracks initially form at regions of local grain boundary separation along die line stress concentrations. Specimens from Zone 2 were tested at both 100 and 80 MPa, and in contrast to the Zone 1 and 4 specimens, exhibited significantly shorter fatigue lives than the Zone 3 specimens. The results from Zone 2 correspond to charge weld separations between 0.5 and 8.0 mm, and there was no obvious trend in fatigue life as a function of charge weld separation, but the effect of charge welds appears to be diminished at lower stress amplitudes (longer fatigue lives).

Results for transverse specimens from the bottom wall (C wall) of the extrusion are also presented in Fig. 8, as open symbols and dashed line. Previous study on Zone 3 of this extrusion showed that the diminution of fatigue life relative to the A wall is associated with increased surface roughness on the C wall, which facilitates fatigue crack nucleation and shortens fatigue life (Ref 5, 11). Those studies also showed that the scatter in fatigue results about the trend line was significantly

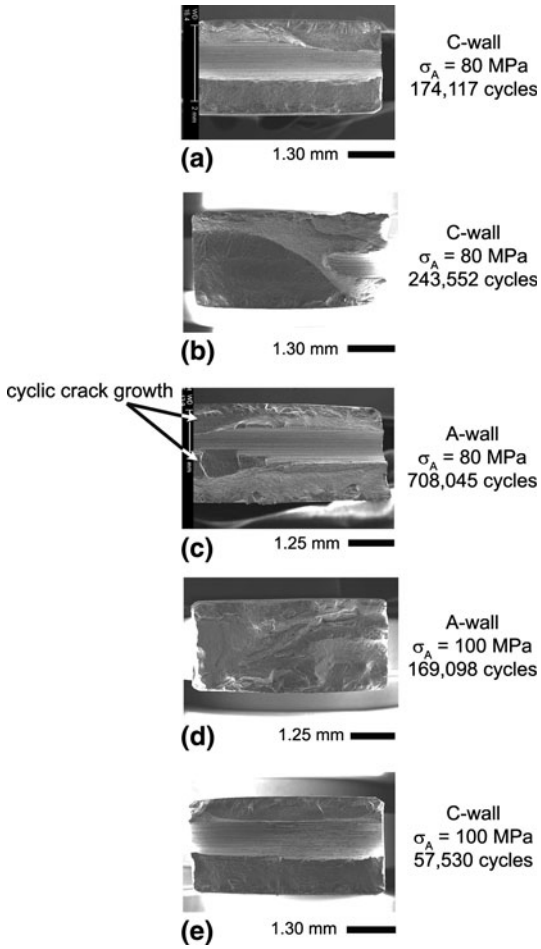

Fig. 9 SEM fracture analysis of several T-CW(2) specimens with charge weld separations near 5 mm

greater for specimens from the C wall than for those from the A wall. The results for fatigue specimens from Zones 1, 2, and 4 fall, for the most part, at or slightly below the Zone 3 trend line, but differences generally fall within the scatterband of results for the C-wall T-W(3).

Figure 9 shows fatigue fracture surfaces of five specimens from the A and C walls of the extrusion profile. All five of these specimens were from Zone 2 and had charge weld separations of approximately 5 mm. In each case, fatigue cracks initiated on the extruded surface and, in all but one fracture surface (Fig. 9d), a portion of the fracture path follows along the charge weld. This implies that in Zone 2, at least one stage of the fatigue failure normally involves failure along the charge weld interface. High-magnification images of the charge weld interfaces showed dimple-type ductile failure, which implies overload failure along the interface instead of striated fatigue crack propagation. Similar fractographic observations on fatigue failures of hollow extruded profiles have been previously observed (Ref 2).

The fractured sample in Fig. 9(e) is also shown in Fig. 10 in cross-section. The crack initiated in the recrystallized layer at the specimen surface, exhibited cyclic crack growth, approximately normal to the applied load, and proceeded until the crack reached the charge weld. Once it reached the charge weld, fast fracture followed along the charge weld interface and then sheared the remaining ligament at approximately 45° to the

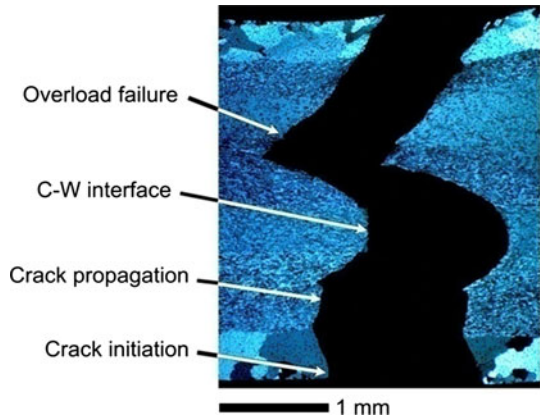

Fig. 10 Optical image of cross-section of T-W(2) specimen (σ_a = 100 MPa, $N_f = 5.7 \times 10^4$) (Fig. 9e) showing typical fatigue failure with crack growth along charge weld interface

loading direction. The failure process in Fig. 9(e) appears to have been nearly identical to that for the sample in Fig. 9(a).

The fracture surface shown in Fig. 9(b) is slightly different than the two mentioned above. The fatigue crack for this specimen initiated below the nose of the charge weld and grew cyclically until the maximum applied load could not be sustained. The specimen then underwent overload shear failure (along a plane inclined approximately 45° relative to loading direction), which intersected and followed the charge weld interface during a portion of overload failure. Figure 9(c) is similar to (a) and (e) except that there is some evidence of cyclic crack growth on both sides of the charge weld interface. The failure at the charge weld interface was dimple-type in this specimen as well; again implying failure along the interface is associated with rapid overload failure rather than cyclic crack propagation.

The fracture surface in Fig. 9(d) does not appear to have followed the charge weld interface at any point during the failure process. In this case, failure appears to have occurred approximately along the seam weld. Crack nucleation and growth at/near the seam weld was not frequent and this specimen is an anomaly.

Based on the fatigue results in Fig. 8, and the fractographic information in Fig. 9 and 10, it appears that decreases in fatigue lives for the T-CW(2) specimens are associated with premature overload failure. In most cases, this overload failure is associated with separation along the charge weld interface. Given that weakness of the charge weld interfaces was not evident in the tensile test results, it seems reasonable to assume that some damage to charge weld interfaces occurred during the cyclic fatigue loading or due to the high local stress concentration at the interface due to the fatigue crack. While there is no direct evidence to support this speculation, it seems likely that this damage (and reduced fatigue life) is associated with strain accumulation at the interface itself or near second-phase particles that are heterogeneously concentrated near the charge weld interface.

5. Discussion

Previous research has clearly documented the important role of die line surface roughness on fatigue performance of

extruded AA6082 aluminum alloy specimens taken from the mid section (Zone 3) of the extruded billet (Ref 5, 11). The results presented here address the influence of charge welds and coring on the fatigue properties of specimens taken from the front (Zones 1 and 2) and the back (Zone 4) ends of extrusion. The effects of the charge welds and coring will be superimposed on the effects of die line roughness, because all the results reported here were for specimens with as-extruded surfaces.

The effect of charge welds is most clearly revealed by comparing results for Zone 2 specimens with the trend lines for Zone 3 specimens. In general, longitudinal specimens from Zone 2 exhibited fatigue properties that are comparable to longitudinal specimens for Zone 3, suggesting fatigue life is not greatly affected by a charge weld oriented parallel to the applied stress, even when the charge weld separation is relatively large.

In contrast to the longitudinal specimens, specimens from Zone 2, oriented transverse to the extrusion direction, generally exhibited fatigue lives lower than those for comparable Zone 3 specimens. The premature fatigue failure of specimens with large charge weld separations was generally associated with some portion of the final overload failure occurring along the charge weld interface. The diminution in fatigue performance for transverse Zone 2 specimens is evident, even though the tensile properties are essentially the same as those for the respective Zone 3 specimens, and tensile failures reveal no evidence of failure along the charge weld interface.

The fatigue lives of these high cycle fatigue specimens is presumably controlled primarily by the time required for fatigue crack initiation. The locations of fatigue crack initiation sites in the transverse, as-extruded, specimens is strongly dependant on surface roughness and locations where deep die line surface features exist. In order for fatigue overload failure to originate along the charge weld interface, a fatigue crack must grow from the initiation site and intersect the weld. Based on the fractographs in Fig. 9 it is clear that this is not always the case for zone 2 specimens, and this undoubtedly adds to the scatter in the fatigue data.

Any effect of coring on fatigue strength in these materials would be evident in comparisons of specimens from Zones 1 and 4 with specimens from Zone 3. Results from specimens from Zones 1 to 4 were not completely consistent. For longitudinal orientations, Zone 4 specimens exhibited somewhat lower fatigue lives at 110 MPa than the Zone 3 specimens. Zone 1 specimens exhibited even larger losses in fatigue strength than the Zone 4 specimens. We note, however, that Zone 1 specimens and to a lesser extent Zone 4 specimens exhibited somewhat lower yield strengths than the Zone 3 specimens, and this diminished yield strength may explain loss in fatigue life. The lower yield strength in Zone 1 could result from aging of the leading billet material as it cooled during butt shearing and billet insertion procedures.

Comparison of fatigue results for transverse specimens from Zones 1 to 4 with the trend lines for Zone 3 generally show mixed results. Some Zone 1 and 4 specimens exhibited longer fatigue lives than the Zone 3 trend line and others exhibited shorter fatigue lives. Keeping in mind that the scatter for transverse Zone 3 specimens from the C wall was considerably greater than for specimens from the A wall, transverse fatigue specimens from Zones 1 to 4 do not appear to be significantly different from the results from transverse Zone 3 specimens.

6. Conclusions

1. The fatigue properties of longitudinal specimens with significant charge weld separations do not appear to be significantly different from the properties in Zone 3 for uniaxial loading.
2. The fatigue properties of transverse specimens from the A wall in Zone 2 appear to be lower than for comparable specimens from Zone 3, and their failures are generally at least in part associated with failure at the charge weld interface. Fatigue properties of transverse specimens from the C wall are generally lower than for the A wall, due to increased roughness of the C wall, and transverse specimens from Zone 2 of the C wall were generally only slightly lower than for those from Zone 3.
3. Billet coring does not appear to have significantly influenced either tensile or fatigue properties in this study. There do appear to be some minor differences between the properties of material from Zones 1, 4, and 3, but they can be explained by effects of billet cooling during butt shearing and billet insertion operations.

Acknowledgment

The authors would like to express their gratitude to Hydro Aluminum, ASA for the support of this research.

References

1. M.P. Clode and T. Sheppard, Formation of Die Lines During Extrusion of AA6063, *Mater. Sci. Technol.*, 1990, **6**(8), p 755–763
2. R. Akeret, Extrusion Welds-Quality Aspects are Now Center Stage, *5th International Aluminum Extrusion Technology Seminar* (Chicago, IL), Vol 1, 1992, p 319–336
3. V. Johannes, C.W. Jowett, and R.F. Dickson, Transverse Weld Defects, *6th International Aluminum Extrusion Technology Seminar* (Chicago, IL), Vol 2, 1996, p 89–94
4. H. Valberg, Extrusion Welding in Aluminum Extrusion, *Int. J. Mater. Prod. Technol.*, 2002, **17**(7), p 497–556
5. N. Nanninga and C. White, The Relationship Between Extrusion Die Line Roughness and High Cycle Fatigue Life of an AA6082 Alloy, *Int. J. Fatigue*, 2009, **31**(7), p 1215–1224
6. V.L. Berezhnoy, K.-H. Hahn, and J.-Y. Chang, Extrusion Defects: Conditions of Formation and Methods of Prevention, *Light Met. Age*, 1999, **57**(3–4), p 66–74
7. A.F.M. Arif, A.K. Sheikh, S.Z. Qamar, M.K. Raza, and K.M. Al-fuhaid, Product Defects in Aluminum Extrusion and their Impact on Operational cost, *6th Saudi Engineering Conference* (Dhahran, Saudi Arabia), Vol 5, 2002, p 137–154
8. T. Hatzenbichler, B. Buchmayr, and A. Umgeher, A Numerical Sensitivity Study to Determine the Main Influence Parameters on the Back-End Defect, *J. Mater. Proc. Technol.*, 2007, **182**(1–3), p 73–78
9. R. Akeret, Properties of Pressure Welds in Extruded Aluminum Alloy Sections, *J. Inst. Met.*, 1972, **100**, p 202–207
10. A. Loukus, G. Subhash, and M. Imaninejad, Mechanical Properties and Microstructural Characterization of Extrusion Welds in AA6082-T4, *J. Mater. Sci.*, 2004, **39**(21), p 6561–6569
11. N. Nanninga, C. White, T. Furu, O. Anderson, and R. Dickson, Effect of Orientation and Extrusion Welds on the Fatigue life of an Al-Mg-Si-Mn Alloy, *Int. J. Fatigue*, 2008, **30**(9), p 1569–1578
12. J. van Rijkom, P.H. Bolt, and D. Weeke, A Review of New Approaches and Technologies in Extrusion Welds Related to the Background of Existing Knowledge, *7th International Aluminum Extrusion Technology Seminar* (Chicago, IL), 2000, p 249–260
13. S. Suresh, *Fatigue of Materials*, Cambridge University Press, Cambridge, 1991